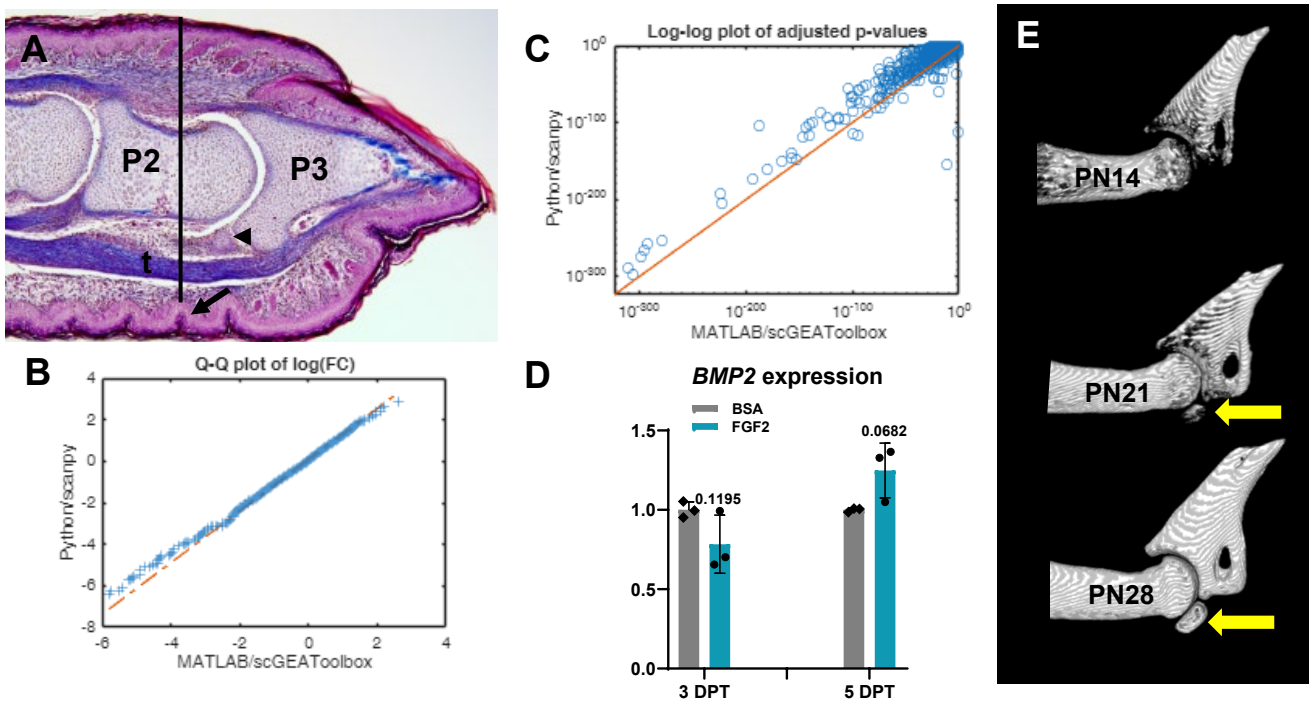

Supplementary Figure 1 – A) Longitudinal section of the neonatal digit at PN3 showing the epidermal folds on the ventral surface. The sub-distal epidermal fold (arrow) was used as a landmark for the mid-P2 (P2) amputation of the digit (line). Note the amputation removed the distal half of the P2 bone, the sesamoid bone (arrowhead) which is just beginning to form in association with a branch of the ventral tendon at this stage, and the entire P3 bone (P3). B,C) Comparison of differential expression analysis results from MATLAB/scGEAToolbox and Python/scanpy. B) Q–Q plot of log fold change (log(FC)) shows strong agreement between the two implementations; each point represents a gene. C) Log–log plot of adjusted p-values indicates close correspondence, demonstrating statistically similar identification of differentially expressed genes. D) qRT-PCR analysis of RNA collected from FGF2 treated P2 amputation at 3 and 5 DPA show that *Bmp2* transcript levels are not enhanced by FGF2 (n=3 biological replicates for each time point). E) µCT imaging shows that ossification of the distal digit sesamoid bone is initiated between N14 and PN21 (yellow arrow) and it is fully differentiated by PN28.

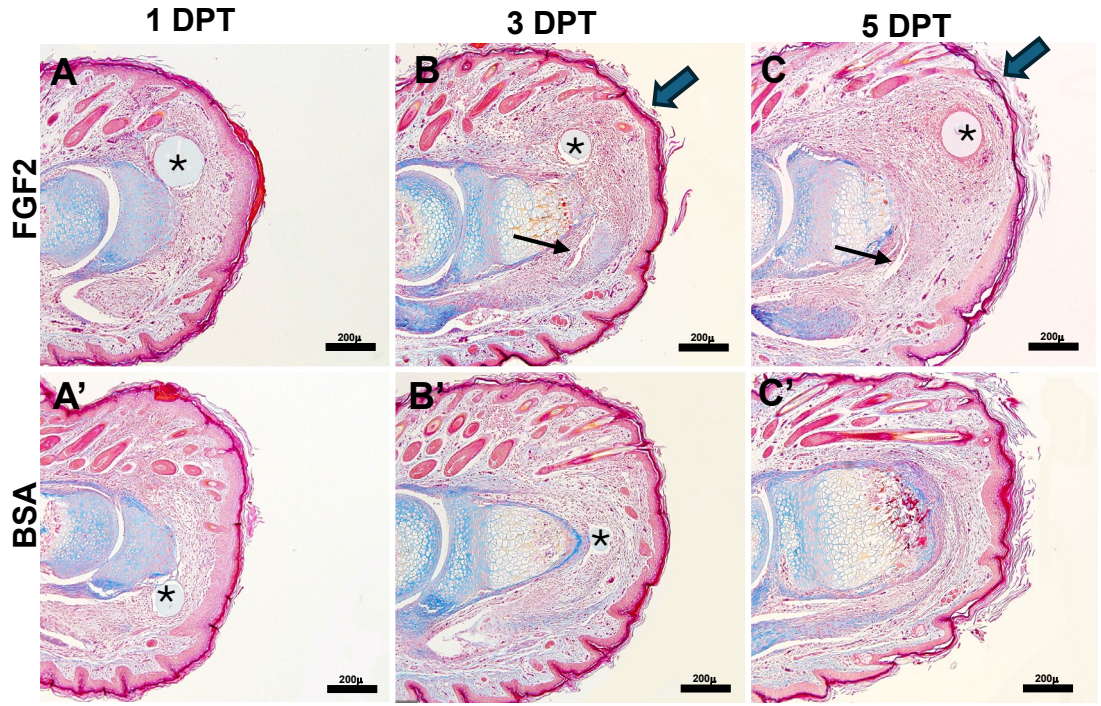

Supplementary Figure 2 – A-C) Progression of FGF2 induced changes of the non-regenerative P2 amputation wound compared to control BSA treated digit amputation. A-A') At 1 day post treatment (DPT) the amputation wound of the FGF2 treated digit (A) does not appear different compared to the control BSA treated digit (A'). B-B') At 3 DPT there is a distinct accumulation of mesenchymal cells associated with the FGF2 bead (*) in the dorsal wound (large arrow) and an ectopic chondrogenic nodule associated with a cavity (small arrow) in the ventral region of the wound (B). The BSA control digit (B') is not modified at 3 DPT. C-C') At 5 DPT the accumulation of cells around the FGF2 bead (*) is pronounced (large arrow) and the joint regeneration response (small arrow) continues in the ventral wound region (C) while the BSA control digit (C') is unremarkable. Sample size for each time point: n=3 digits.

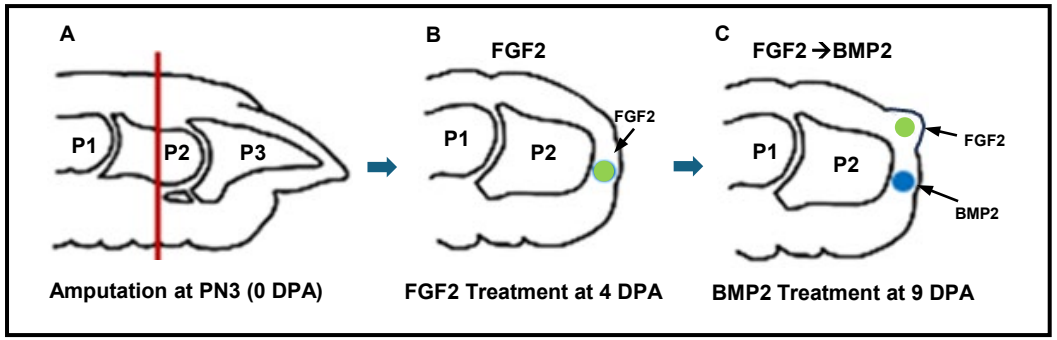

Supplementary Figure 3 - Experimental design for sequential FGF2 and BMP2 treatment (FGF2→BMP2) of the amputated digit. A) The digit is amputated on PN3 midway through the P2 bone. B) 4 days post amputation (4 DPA) the amputation wound is closed and an FGF2 bead is implanted into the amputation stump. C) 5 days later (9 DPA) a blastema forms in the distal-dorsal region of the amputation wound and a BMP2 bead is implanted into the center of the amputation stump. This figure was created by Ling Yu and modified by Ken Muneoka using powerpoint.

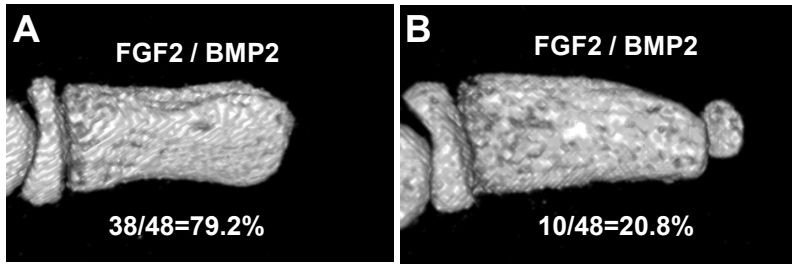

Supplementary Figure 4 – Administration of FGF2 and BMP2 simultaneously after wound closure (4 DPA) results in a response similar to FGF2 treatment alone. 79.2% of the digits are truncated (A) and 20.8% of the digits formed a distal ectopic skeletal element (B).

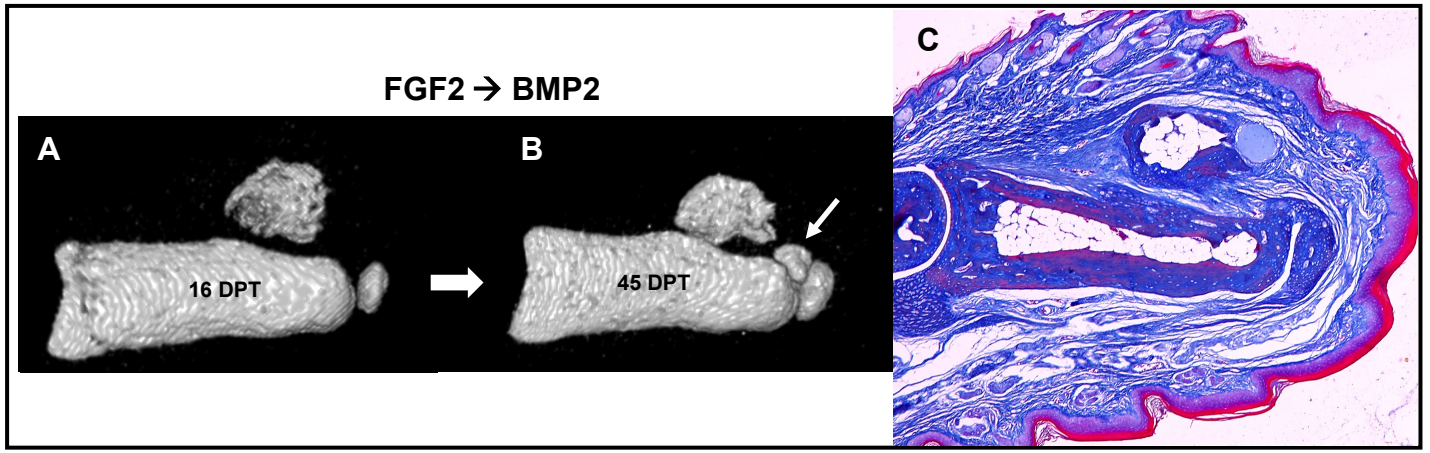

Supplementary Figure 5 – FGF2→BMP2 treated digit amputation that regenerated 3 ectopic skeletal elements at 45 days post treatment (DPT); one large element dorsal and two smaller distal elements. A) At 16 DPI 2 ectopic elements were observed by μCT; a large dorsal element and a small flattened distal element. B) At 45 DPI, a third element (arrow) formed between the stump and the distal element. C) Histological analysis showed that the dorsal element had a large marrow cavity whereas the flattened distal element was associated with a joint cavity.

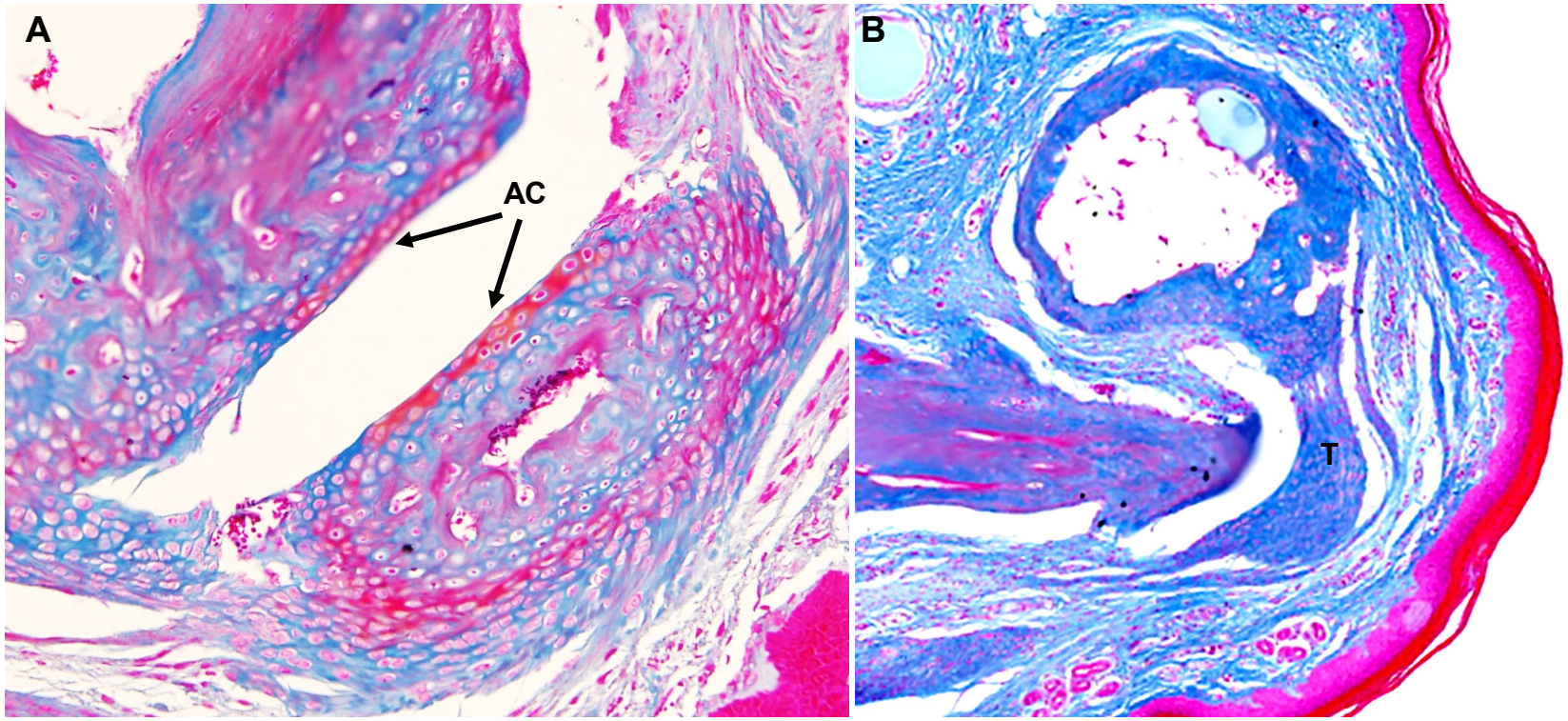

Supplementary Figure 6 – A) Histological evidence of articular cartilage (AC, arrow) regeneration lining the regenerated cavity on both stump and ectopic bone surfaces in a FGF2→BMP2 treated digit amputation that regenerated a dorsal and a distal-ventral ectopic skeletal element at 45 days post treatment. B) Histological evidence of a tendon (T) that regenerated from ventral tissue over the P2 stump bone and attached to the single dorsal ectopic bone induced to regenerate 45 days after FGF2→BMP2 treatment.

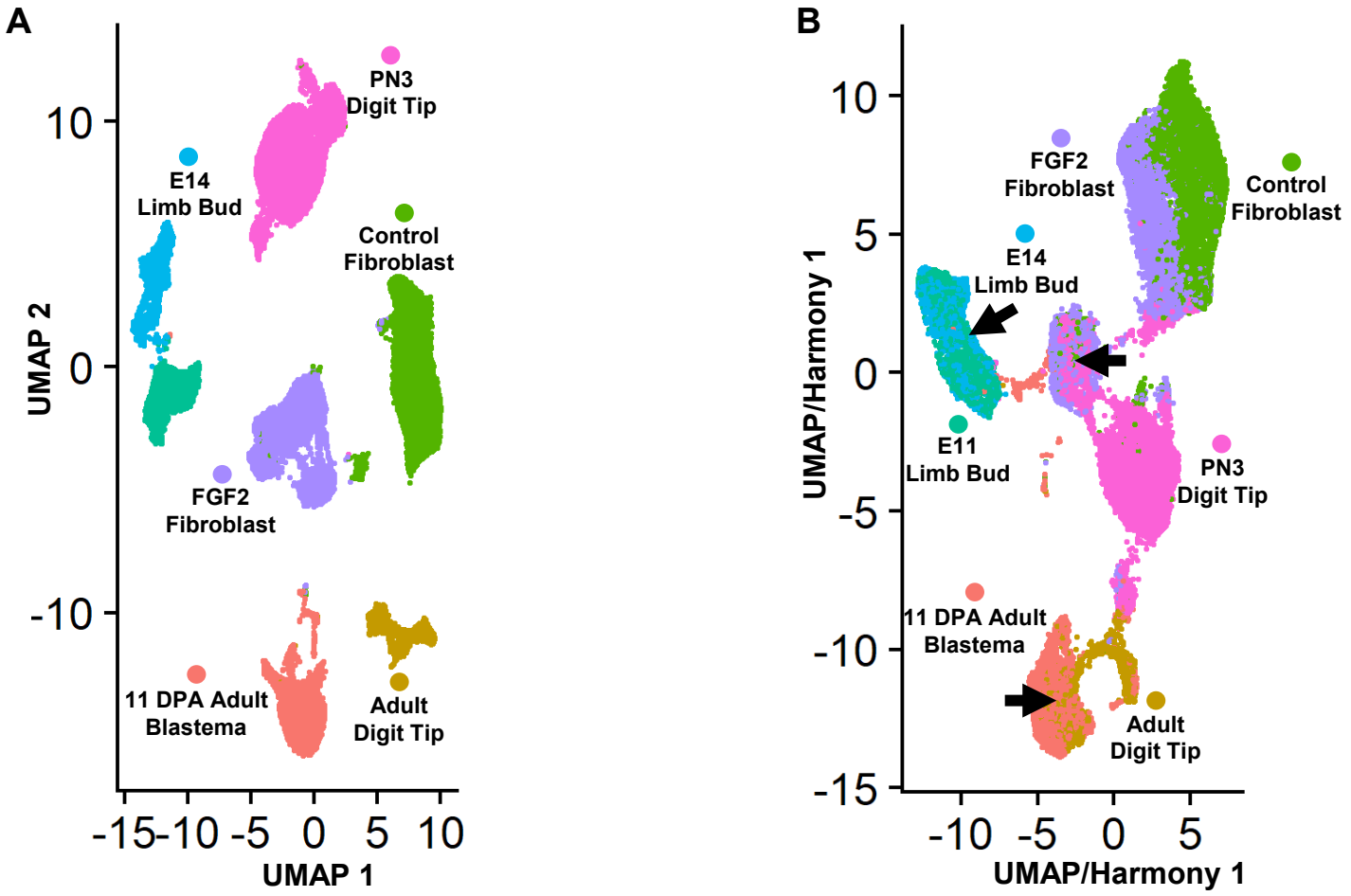

Supplementary Figure 7 – A) 2-dimensional UMAP projection generated using Seurat/R of fibroblast-specific datasets from embryonic day 11 (E11) and E14 limb buds, the unamputated digit tip at PN3, the unamputated adult digit tip (43; GSE135985) and the adult digit tip blastema at 11 days post amputation (dpa) (52; GSE143888) for comparison to datasets generated from control and FGF2 treated amputation wound fibroblasts. B) The UMAP projection was also generated following Harmony-based batch correction to highlight overlapping cellular subpopulations between conditions. Overlapping cell subpopulations (arrows) exist between E11 and E14 limb bud fibroblasts, between FGF2 treated neonatal amputation wound fibroblasts and neonatal (PN3) digit tip fibroblasts, and between adult 11 dpa digit blastema fibroblasts and adult digit tip fibroblasts.

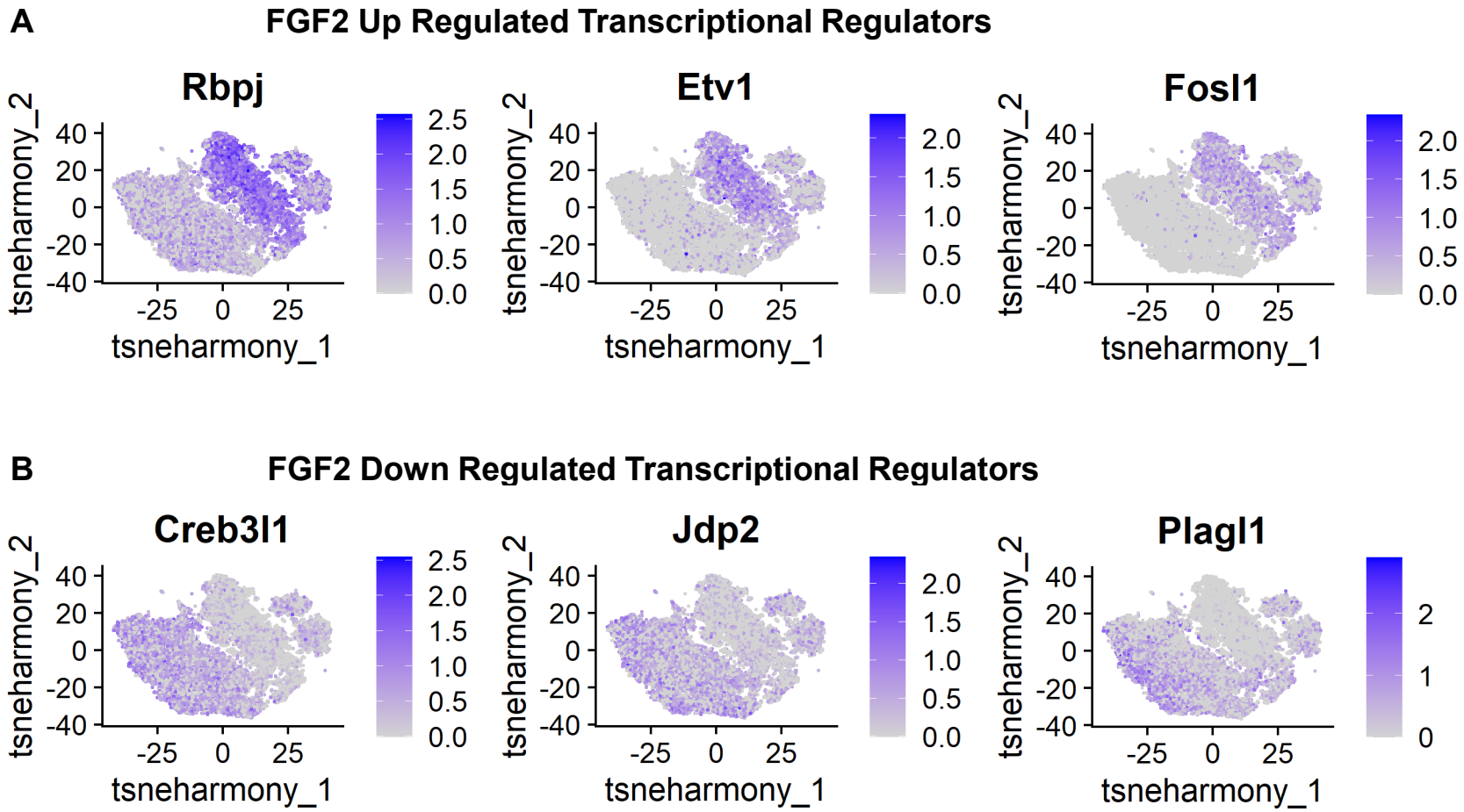

Supplementary Figure 8 – Seurat FeaturePlots of normalized expression projected onto the Harmony-integrated t-SNE embedding. A) 3 genes of transcriptional regulators are up regulated in the majority of FGF2 treated cells and expressed at low levels in untreated control cells. B) 3 genes of transcriptional regulators are express in the majority of untreated control cells and are down regulated in FGF2 treated cells.

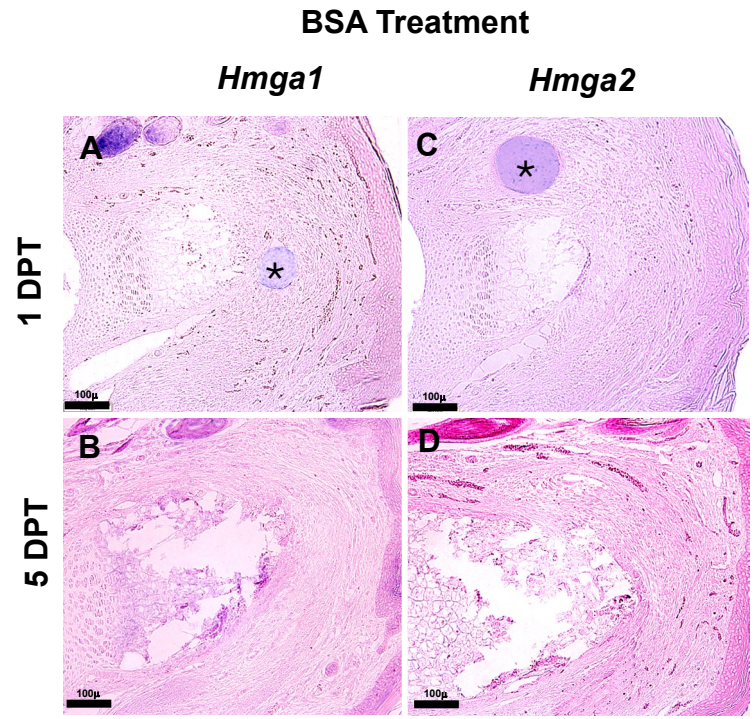

Supplementalry Figure 9. Control *in situ* hybridization to localized *Hmga1* (A,B) or *Hmga2* (C,D) transcripts on paraffin sections of digit amputation wounds 1 day (A,C) and 5 days (B,D) after BSA bead (*) implantation. *Hmga1* and *Hmga2* transcripts were not expressed in control amputation wounds that heal by fibrosis. Sample size for each gene/timepoint: n=4 digits.

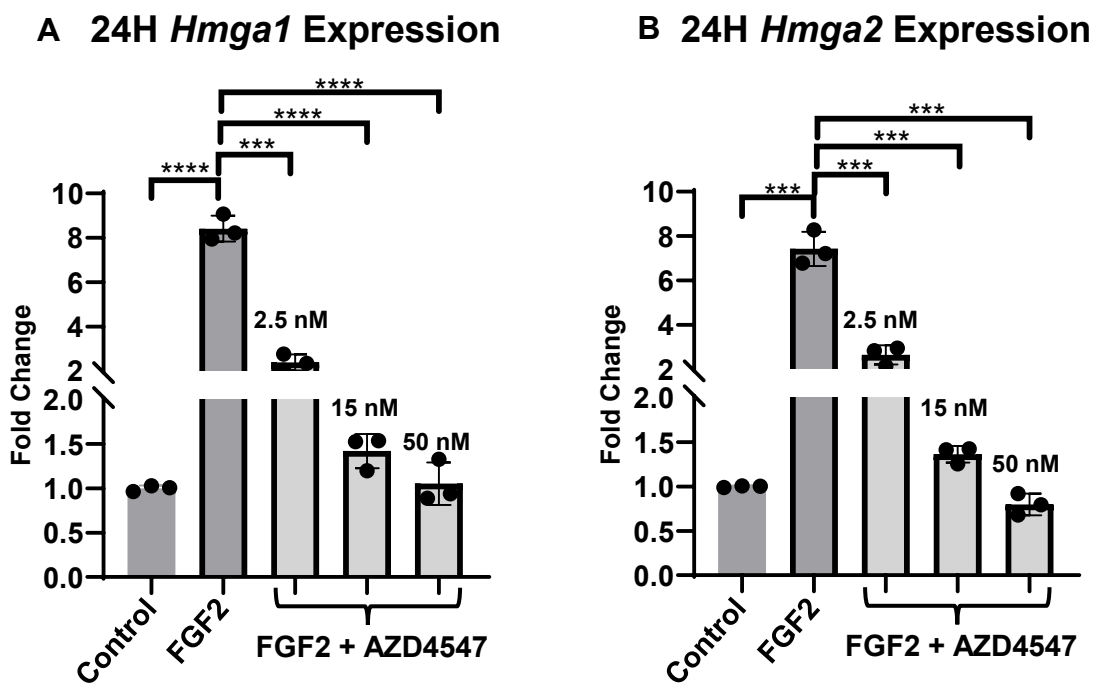

Supplementary Figure 10 – FGFR inhibition studies**.** Pre-treatment of cultured amputation wound fibroblasts with the pan FGF receptor inhibitor, AZD4547 (Selleck Chem LLC) blocks the induction of *Hmga1* (A) and *Hmga2* (B) induced expression by FGF2 (100 ng/ml) in a dose-dependent manner at 24 hours. N=3 biological replicates for each dose. ***P<0.001; ****P<0.0001.

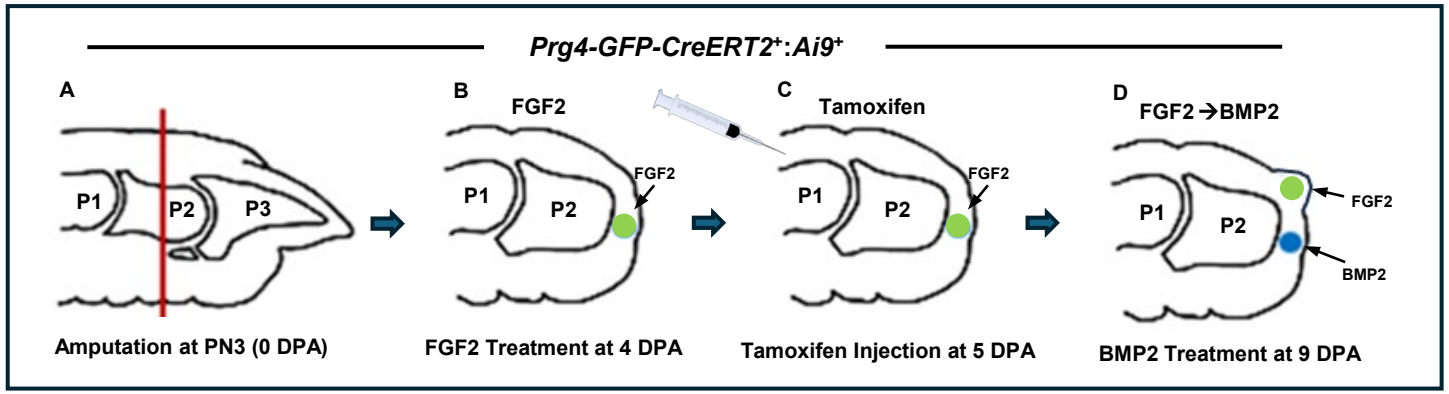

Supplementary Figure 11 - Experimental design for tamoxifen treatment of FGF2→BMP2 treated amputated digits of *Prg4-GFP-CreERT2*$^{+}$:*Ai9*$^{+}$ neonatal mice. A) The digit is amputated midway through the P2 bone at PN3. B) 4 days after amputation (4 DPA) the amputation wound is closed and an FGF2 bead is implanted into the amputation stump. C) 1 day later (5 DPA) tamoxifen is injected systemically to induce *tomato* expression (TdT) in *Prg4* expressing cells. D) 4 days later (9 DPA) a BMP2 bead is implanted into the center of the amputation stump. This figure was created by Ling Yu and modified by Ken Muneoka using powerpoint.

Supplementary Note 1 - FGF2 Differentially Expressed Genes

Genes Up Regulated by FGF2: *AA467197, Abcb1a, Abcb1b, Adam8, Adora2b, Adssl1, Aif1l, Akr1c18, Aldh1a3, Ank, Anln, Ano3, Aox1, Apcdd1, Aqp1, Arap2, Arhgap22, Arhgap6, Arl4c, Ass1, Baiap2l1, Bcl2l1, Birc5, Bmp2, C77080, Camk1d, Ccdc3, Cck, Ccl2, Ccnb1, Ccnb2, Ccnd1, Ccnf, Cd34, Cd44, Cd80, Cdt1, Cenpf, Chic1, Chrna1, Chst1, Clcf1, Cldn11, Cldn15, Clic5, Cplx2, Cx3cl1, Cyb561, Cyp2f2, Cystm1, Ddias, Diaph3, Dio2, Dlgap1, Dnph1, Dok1, Dusp10, Dusp5, Dusp6, E2f8, Eda2r, Egr3, Eml5, Entpd1, Epha2, Eps8, Ercc1, Ereg, Erich2, Ermp1, Errfi1, Esm1, Etv1, Etv4, Eva1c, Fam111a, Fam181b, Fam78b, Fez1, Fjx1, Flrt1, Fosl1, Foxl1, Frzb, Gask1b, Gch1, Gchfr, Gdf6, Gldn, Gprc5a, Gsdme, Gss, Gtse1, Hectd2, Hmga1, Hmga1b, Hmga2, Hmmr, Igsf9b, Il11, Il16, Il18rap, Il6ra, Inf2, Inka2, Iqgap2, Itga4, Itga6, Itgb2, Itgb3, Itgb4, Itgb7, Itpr3, Kcnn4, Kctd4, Kifc1, Klf10, Klf5, Klk8, Lbhd2, Lgr6, Lipg, Lmo2, Lrp8, Map3k6, Mapk13, Mbnl3, Mcm5, Mcpt8, Mcub, Mdm2, Met, Mfap3l, Mfsd6, Mgat5, Mtcl1, Mthfd1l, Mybl1, Myzap, Nav2, Nav3, Nceh1, Nes, Neto2, Notum, Nppc, Nptx1, Nrcam, Nxph3, Odc1, Orai2, Osbpl3, Pakap, Parvb, Pbld1, Pclaf, Pdzd2, Perp, Phlda1, Pi16, Pidd1, Pla2g7, Plau, Plaur, Plcg2, Plk3, Pmaip1, Prc1, Prkcb, Prkg2, Prl2c2, Prl2c3, Prrg4, Ptchd4, Ptger1, Ptges, Ptgir, Ptgs1, Ptgs2, Ptk2b, Ptpn22, Ptprn, Pxn, Rab3b, Rai14, Ramp3, Rapgef3, Raph1, Rassf3, Rbm47, Rbpj, Rem1, Rgmb, Rin1, Ripk3, Rrm2, S100a3, S100a7a, S100a8, Samd12, Schip1, Sema4b, Sema7a, Serpinb2, Sgms1, Sgms2, Sh3bgrl2, Slc14a1, Slc16a1, Slc16a11, Slc19a2, Slc20a2, Slc25a37, Slc43a2, Slco2a1, Smox, Spink2, Spred2, Spred3, Spry4, Stn1, Stom, Syngr1, Sytl1, Tbc1d2, Tcim, Tes, Tiam1, Tinagl1, Tm4sf1, Tmem200a, Tmem47, Tmem51, Tnfrsf12a, Tor4a, Tpd52, Trbc2, Trem2, Trib2, Trim7, Trpm6, Tslp, Tspan15, Ube2c, Ubtd1, Uhrf1, Unc13c, Upp1, Vldlr, Wnt10a*

Genes Down Regulated by FGF2: *Abi3bp, Acot2, Acta2, Acvr2a, Adam12, Adamts15, Adamts9, Adamtsl1, Adh1, Aff3, Agtr1a, Aldh1l2, Ankrd55, Arhgap20, Armh4, Aspn, Bcl11a, Bdh2, Bend5, Cadm2, Ccdc30, Ccdc80, Cd24a, Cdc42ep3, Cdkl5, Cdkn1c, Cdon, Chodl, Clec11a, Clec3b, Cmbl, Col11a1, Col12a1, Col27a1, Creb3l1, Cthrc1, Cttnbp2, Cxcl12, Cxcl15, Cybrd1, Cys1, Dact1, Dapk1, Ddr1, Ddx4, Dipk1a, Dipk2a, Dlc1, Dleu2, Dnajb3, Dpep1, Ecrg4, Efs, Egfl6, Eln, Epha3, Epha4, Epha5, Eya4, Fat4, Fbln7, Fbn2, Fbxl7, Fgfr2, Fgl2, Fhl1, Fibin, Fmo1, Fmod, Fndc1, Fndc4, Foxp2, Fxyd1, Fzd4, G0s2, Gadd45b, Gadd45g, Galnt13, Galnt9, Gas2, Gdf10, Gdpd2, Ggt5, Gstt1, Gucy1a1, Gulp1, Hmcn1, Hpgd, Hpse2, Hspb2, Htra3, Id4, Igf1, Igfbp2, Igfbp5, Il1r2, Islr, Ism1, Jdp2, Kera, Klhl13, Lbp, Ldb2, Lgalsl, Limch1, Lmcd1, Lpl, Lrig3, Lrrc17, Lypd1, Maml2, Matn4, Mcc, Me3, Megf6, Mest, Mex3b, Mfap4, Mia, Mmp11, Myl9, Mylk, Ncam2, Nckap5, Nedd9, Nhsl1, Nid2, Nkd1, Nrep, Nuak1, Ogn, Olfml1, Omd, Ophn1, Otulinl, Pappa, Parm1, Pcsk5, Pdgfd, Pdgfrl, Pdk1, Phactr1, Phyhd1, Plagl1, Plcxd2, Plekhf1, Plscr2, Podn, Podxl2, Porcn, Ppfibp2, Ppp1r3b, Prelp, Prlr, Prr16, Prss23, Prss35, Pth1r, Ptn, Ptprd, Ptx3, Pygo1, Rab30, Ramp1, Rasl11a, Rbp4, Reps2, Rgs4, Ripor3, Rnf144a, Robo2, Rspo2, Rspo3, Sbspon, Sema3d, Serpine1, Sfrp1, Sfrp2, Shroom3, Slc1a3, Slc1a6, Slc24a3, Slc40a1, Slc9a9, Smarca1, Smoc1, Smpdl3a, Sorcs2, Srpx, St8sia2, Steap4, Susd2, Svep1, Tbxa2r, Tceal3, Tcerg1l, Tenm3, Tent5a, Tgfb2, Thsd7a, Tmeff1, Tmem26, Tnik, Tnn, Trib3, Unc5c, Vipr2, Vstm4, Wnt16, Wnt5b, Ypel1, Zfp521*

Supplementary Table 1. Primer information for qRT-PCR

Name primer		Sequence information	Name primer		Sequence information
1	*Mouse Ccl2*	Mm00441242_m1	2	*Mouse Cxcr4*	Mm01996749_s1
3	*Mouse Cxcl12*	Mm00445553_m1	4	*Mouse Msx1*	Mm00440330_m1
5	*Mouse PDGFrα*	Mm00440701_m1	6	*Mouse TGFβ1*	Mm01178820_m1
7	*Mouse Col2a1*	Mm01309565_m1	8	*Mouse Col10a1*	Mm00487041_m1
9	*Mouse Lmx1b*	Mm00440209_m1	10	*Mouse Hoxa13*	Mm00433967_m1
11	*Mouse Hoxd13*	Mm00433973_m1	12	*Mouse Prg4*	Mm01284582_m1
13	*Mouse Hmga1*	Mm01302616_g1	14	*Mouse Hmga2*	Mm04183367_g1
15	*Mouse RPL12*	Mm02601627_g1			

Supplemental Table 2 – Notable Limb Development Genes Differentially Modified by FGF2 Treatment

gene	Log_2FC	FGF2 (%)	Ctrl (%)	Adj P Value*
FGF2 Up Regulated				
Etv4	5.60	28.2%	0.5%	0
Lgr6	4.87	13.6%	0.5%	0
Frzb	4.51	27.0%	1.3%	0
Spry4	4.21	60.8%	3.9%	0
Notum	3.66	21.7%	1.6%	0
Etv1	2.78	82.3%	16.5%	0
Bmp2	1.76	37.6%	13.4%	0
Cd34	1.76	70.5%	24.6%	0
Ptchd4	1.72	9.1%	2.4%	7.069E-103
Cd44	1.70	86.8%	33.6%	0
Gdf6	1.68	11.6%	3.5%	2.1153E-115
Wnt10a	1.60	20.1%	6.8%	8.1746E-183
FGF2 Down Regulated				
Gdf10	-3.80	3.5%	30.6%	0
Igf1	-3.79	8.8%	59.8%	0
Igfbp5	-3.57	11.3%	69.4%	0
Fmod	-3.25	2.5%	13.2%	7.7815E-160
Pth1r	-3.20	2.3%	16.2%	1.415E-223
Sfrp2	-2.96	20.7%	71.9%	0
Wnt16	-2.61	14.5%	53.0%	0
Tgfb2	-2.27	22.9%	62.2%	0
Wnt5b	-2.17	6.9%	21.0%	4.8851E-186
Matn4	-2.05	6.0%	15.9%	8.0377E-111
Fzd4	-1.97	6.3%	16.7%	2.7424E-120
Acvr2a	-1.95	15.0%	36.7%	0
Fgfr2	-1.94	17.5%	41.4%	0
Pdgfrl	-1.93	41.5%	82.5%	0
Mest	-1.57	14.7%	31.6%	9.4234E-198
Cxcl12	-1.56	78.0%	99.5%	0
Pdgfd	-1.53	12.0%	23.5%	2.6396E-121
Sfrp1	-1.52	52.6%	75.6%	0

*Differential gene expression between the two groups of cells was assessed using a two-sided Wilcoxon rank-sum test. Resulting P values were adjusted for multiple comparisons using the Benjamini–Hochberg false discovery rate (FDR) procedure, and the adjusted values are reported as FDR-corrected P values.